

Experimental and Theoretical Studies of the Molecular Motions in Polymer Crazing. 1. Tube Model

H. Z. Y. Han,[†] T. C. B. McLeish,^{*,†} R. A. Duckett,^{*,†} N. J. Ward,[‡] and A. F. Johnson[‡]

Interdisciplinary Research Centre in Polymer Science and Technology, Department of Physics and Astronomy, and School of Chemistry, University of Leeds, Leeds, LS2 9JT, U.K.

A. M. Donald and M. Butler

Cavendish Laboratory, University of Cambridge, Madingley Road, Cambridge, CB3 0HE, U.K.

Received December 26, 1996; Revised Manuscript Received December 8, 1997

ABSTRACT: A theoretical model has been developed to calculate the craze surface energy for monodisperse linear polymers based on the “tube model” of polymer melts. This model, which is a refinement of models previously proposed, assumes that the essential molecular processes of chain scission and disentanglement occur in the “active zone”—a region of thickness greater than or equal to the chain radius of gyration, situated at the interface between craze and bulk polymer. At high temperatures, greater than a critical temperature, $T > T_{tr}$, craze growth occurs by stress-assisted chain disentanglement; below a second critical temperature, T_{cr} , craze growth occurs by chain scission. Between these critical temperatures, which are molecular weight and strain-rate dependent, craze growth involves both scission and disentanglement. New experimental data on craze growth in monodisperse, linear polystyrene over a range of temperatures at two strain rates are presented, which are well described by the new theory. The theory describes all features of the data with only one fitting parameter, including small peaks observed in the crazing strain/temperature graphs in the mixed-mode region. Similar features have been reported recently in craze data from poly(methyl methacrylate) without explanation.

Introduction

The single chain pull-out mechanism is very important in many failure processes of amorphous polymers such as in the break down of an adhesive joint,^{1–4} the bulk fracture of glassy polymers,⁵ and the failure at the interface of two immiscible polymers joined by a diblock copolymer.^{6,7} The last process has potential for industrial application and has recently attracted much research interest.

The chain pull-out mechanism has also been associated with the craze growth process in glassy polymers.^{4–6,8–11} The differences between various chain pull-out models have been summarized thoroughly by Brown.⁴ Interesting physics has been discovered in single chain pull-out studies, such as the “suction” process proposed by de Gennes at weak adhesive junctions.¹ In 1983 Prentice tried to apply the tube model to the fracture of solid polymers in glassy states.⁷ In 1987, Berger and Kramer suggested that reptation may be important in the crazing behavior of glassy polymers below their glass transition temperatures.⁸ In 1989, McLeish, Plummer, and Donald applied the tube model to crazing and built up a molecular model for crazing.⁹ Forced reptation was considered and a “block-and-tackle” mechanism was proposed to calculate the chain contour length velocity. The followup paper by Plummer and Donald¹⁰ linked the frictional forces acting on a single chain to the change in crazing mechanisms and predicted the general features of the craze growth surface energy. However, inadequate quantitative agreement between the theory and experiment left room for improvement. It also implied that underlying physical principles needed to be clarified in the crazing behaviors of glassy polymers.

In this paper, experiments have been designed for comparison with both the previous theories and the theory developed here. Monodisperse linear polystyrene with a radius of gyration close to the craze fibril spacing was synthesized so that the molecular weight distribution does not need to be considered. The time scale and strain rate of stretching experiment were designed to be in a clearly defined range, so that the experimental results could be directly compared to the theoretical calculations.

A general tube model for crazing in glassy polymers with a monodisperse molecular weight distribution, below their glass transition temperatures, is introduced. We use entanglement instead of crossing molecular weight¹⁰ as the basic element of the tube as in a conventional tube theory. This tube model for crazing is no longer restricted to chains tied between two separating planes. Changes made from the previous tube model for crazing^{9–11} also include the following: first, the dependence of the critical temperature on the lower cutoff in the fragment molecular weight distribution, second, the role of chain retraction in disentanglement, and, third, the probability of scission in the mixed crazing regime.

On the basis of the generalized tube model for crazing, we have developed a discrete model to address some aspects of the craze growth process. Using the discrete model, we found that previous theoretical calculations provided the upper boundary of the craze growth surface energy. The genuine disentanglement energy can be calculated from the actual fragment molecular weights instead fragment molecular weights M_{crit} and $M_{crit}/2$ as previously used and suggested, respectively.¹⁰

In the second paper of this series to follow,¹² more experimental data from monodisperse linear and three-arm star polystyrenes with different molecular weight

[†] Department of Physics and Astronomy.

[‡] School of Chemistry.

are presented. The current theory is expanded to incorporate center of mass motion under an inhomogeneous stress field and molecular topology.

Experimental Section

Monodisperse linear polystyrene (polydispersity index 1.04) with an M_n (number average molecular weight) of 110 000 (L110k, L means linear, 110k the molecular weight) was synthesized via anionic polymerization. Thin polystyrene films (around 400 μm in thickness) were made by dipping a glass slide into a 5 wt % toluene solution and withdrawing it at a constant speed of 1 cm/min. The film was floated off in a water bath after the solvent had evaporated and subsequently picked up by a copper mesh previously coated with a diluted solution. After the sample was dried overnight, the film was bonded to the copper grid by heating for 10 min at 125 °C under nitrogen. The sample was then aged for 12 h at 80 °C in a nitrogen atmosphere. The final film is about 250 μm thick. The stretching experiment was carried out on a Miniature Material Tester (Polymer Laboratories) at strain rates of 10^{-3} s^{-1} and 10^{-4} s^{-1} in a temperature-controlled cell. A microscope was used to monitor the stretching process, and the strain at which a craze occurred was recorded. The stretching experiments were repeated at least 8 times, and the error is within 15% for each drawing condition.

Basic Model

A polymer craze may be formed by two possible mechanisms:^{9–11} chain disentanglement or scission. The chain will disentangle without breaking when the frictional force acting on the chain is not strong enough to break it. The chain will break when the maximum frictional force acting on the chain, f_{max} , increases (either by decreasing the drawing temperature or increasing the strain rate) to be equal to the constant F , the force required to break the chain.

We assume, following previous authors,^{9–11} that the essential molecular processes of chain stretching, scission and disentanglement occur within an “active zone” situated at the craze–bulk interface and parallel to it. The active zone is wide enough to mobilize entire molecules as it is of comparable or larger width than a typical radius of gyration.¹¹ High stresses in this zone allow the mobilizing of molecular motions normally absent below T_g . For molecules drawn into craze fibrils by a passing craze, their passage through the active zone thus resembles in some ways a polymer melt flow: there is a local high strain field requiring molecular motion (or scission), and the large-scale motions are dominated by entanglements. We used the tube model to treat their consequences. This was done by Kramer and Berger,¹¹ but rather than considering as they do a *separating plane* across which molecules must disentangle or break, we consider the active zone as an inhomogeneous flow field in which the craze fibrils act as “sinks”. We will see that these pictures are nearly equivalent.

A craze active zone differs from a normal polymer melt in that its mobility arises from high molecular stresses rather than Brownian motion with “free-volume” above T_g . So relaxation from a strained state will necessarily be incomplete (chains are still highly oriented in the glassy craze fibrils emerging from the active zone). We will build this immobilization into our model for the molecular stretch relaxation.

A key consideration is the significance of the “center-of-mass” motion of the chains. By this we mean the *curvilinear* motion along the tube contour of the central monomer of a chain (we define “center-of-mass” in a

1-dimensional curvilinear sense, rather than a 2-dimensional one). In a spatially uniform flow-field (uniform over at least a molecular radius of gyration) and for sufficiently long chains this will be close to zero as each half of the chain is subjected to identical stretching by the flow.¹³ In this paper we assume that these limiting conditions are satisfied, and defer treatment of the effects of nonzero center-of-mass motion to the following paper.

In the current tube model, a velocity profile along the chain contour length is first proposed. On the basis of this velocity profile, the frictional force acting on a chain is calculated. To disentangle a chain, the frictional force has to be overcome. It is clear that the magnitude of f_{max} determines whether the chain breaks or not. The average force acting on a chain, f_{av} , can be used to calculate the energy needed to disentangle it.

Considering a chain with two ends moving toward the two adjacent craze fibrils in the craze widening process, we put the origin at the center of mass of the chain. The relative local velocity v of the chain to its surroundings (modeled by the tube) at a certain point s along the contour of the chain is approximately

$$v = ks \quad (1.1a)$$

where the velocity constant k relates to the craze interface separation rate and scales with the strain rate of the tensile experiments.^{9,10} The k value can be shown to depend on the orientational average of chain fragments $\langle uu \rangle$ as follows:

$$k = K \langle uu \rangle \quad (1.1b)$$

where K is the deformation rate tensor and u the unit vector (p 275 of ref 13). In the uniform-field approximation used in this paper, k should be taken as an average over the molecule as it passes through the active zone. Formula 1.1 is not restricted to chains tied between separating planes. The force acting on the point s is accumulated from the near end of the chain to that point

$$f(s) = \int_s^{\pm L/2} \zeta k x \, dx, \quad 0 \leq |x| \leq L/2 \quad (1.2)$$

where ζ is the dynamic monomer friction coefficient and L is the equilibrium tube length. It is worth noting that this velocity profile implies that the maximum frictional force is at the chain center. It is calculated to be

$$f_{\text{max}} = \frac{1}{8} \zeta k L^2 \propto n_e^2 \quad (1.3)$$

where n_e is the number of entanglements per chain. The average frictional force in the chain can be calculated similarly:

$$f_{\text{av}} = \frac{1}{12} \zeta k L^2 \propto n_e^2 \quad (1.4)$$

Formula 1.3 shows that f_{max} relates to strain rate through the velocity constant k and to temperature through the dynamic monomer frictional coefficient ζ . The maximum force acting on a chain can be considered to be a constant at a given drawing condition (temperature and strain rate) and the overall orientation of the chain. The above formulas, (1.3) and (1.4), also imply

that the frictional force acting on the chain is proportional to the square of the number of entanglements per chain.

Transition and Critical Temperatures

We suppose that the force required to break the main chain and the monomer friction coefficient in the melt, as used by Kramer and Berger¹¹ in the craze active zone, are given respectively by:

$$F = \frac{U}{2b} \quad \zeta = Ae^{E/RT} \quad (2.1a)$$

where U is the energy required to break the backbone chain and b is the monomer unit length. A is the "infinite-temperature limit" of the friction coefficient.

At a given strain rate and temperature, there is a specific entangled path length (L_{crit}) or molecular weight (M_{crit}), for which the maximum frictional force equals the force needed to break the chain. Chains longer than the critical path length L_{crit} will break and shorter chains will not. As in the approach of Kramer and Berger⁸ the critical values can be calculated by combining (1.3) and (2.1a) to be

$$L_{\text{crit}} = 2\sqrt{\frac{U}{bAke^{E/RT}}} \quad M_{\text{crit}} = \frac{L_{\text{crit}}}{b}\sqrt{M_e M_0} \quad (2.1b)$$

M_{crit} , the critical molecular weight, has a clear physical meaning here and a definite value at a given drawing condition. It is used to predict the transition in the craze growth mechanism for a molecule of given chain length. The expression for M_{crit} arises from writing the path length L of the molecule as the number of entanglement segments (M/M_e) times the length of an entanglement segment, $b(M_e/M_0)^{1/2}$, where M_0 is the monomer mass. L is the molecular contour coarse-grained at the scale of an entanglement length.

As expected at a given temperature, the critical chain length is shorter at higher strain rates. At a given strain rate, the critical chain length increases as the temperature increases. This is because the frictional force on the chain decreases as temperature rises and it is easier for the chains to disentangle at higher temperatures.

For a molecule of a given chain length, at a given strain rate, f_{max} equals F at temperature T_{tr} . Combining (1.3) and (2a), the transition temperature at which the crazing mechanism changes from that of a pure disentanglement to a mixed scission and disentanglement crazing mechanism is calculated to be

$$T_{\text{tr}} = \frac{E}{R \ln\left(\frac{4U}{bkAL^2}\right)} \quad (2.2)$$

Above T_{tr} , crazes grow by pure disentanglement. T_{tr} is the highest temperature where scission can take place. Below T_{tr} , crazes grow by mixed scission and disentanglement mechanisms.

Previous investigations¹⁰ assumed that when the critical molecular weight (M_{crit}) is below $2M_e$, the craze grows by chain scission only and there is no energy consumed in chain disentanglement. The argument was that when the critical molecular weight is $2M_e$ the broken chain segment molecular weight would be less than M_e which by definition cannot entangle thus

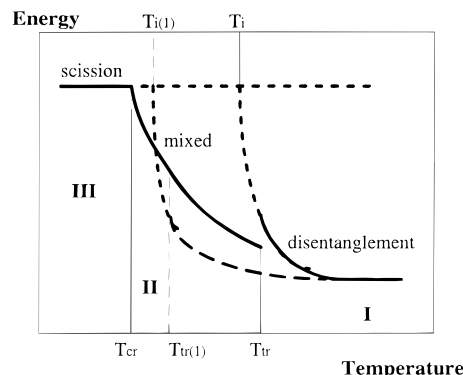


Figure 1. Polystyrene crazing mechanisms: $T < T_{\text{cr}}$, pure scission; $T > T_{\text{tr}}$, pure disentanglement; $T_{\text{cr}} < T < T_{\text{tr}}$, mixed regime. Craze growth surface energy: high molecular weight (thick solid line); low molecular weight (thick broken line). Energy balance for pure disentanglement and pure scission is given by thick dotted lines. Transition temperature: high molecular weight (T_{tr}); low molecular weight ($T_{\text{tr}(1)}$). Critical temperature (T_{cr}). Transition temperature from energy balance: high molecular weight (T_i); low molecular weight ($T_{i(1)}$).

cannot disentangle. However, at the critical temperature predicted by previous theory (calculated by M_{crit} equals $2M_e$), fragments with molecular weights higher than M_e but lower than $2M_e$ will not break, and energy has to be consumed to disentangle these fragments but was omitted from the calculations. In this paper we argue that since work is required to disentangle fragments of molecular weight M_e and above, pure scission crazing occurs only when the critical molecular weight is equal to or less than M_e .

When the chain length equals one entanglement length (*i.e.*, $L = a$, the equilibrium tube diameter), crazes grow by pure scission at temperatures lower than a critical temperature (T_{cr}). For longer chains, mixed mode crazing occurs for $T_{\text{cr}} < T < T_{\text{tr}}$. The critical temperature can be calculated from

$$T_{\text{cr}} = \frac{E}{R \ln\left(\frac{4U}{bkAa^2}\right)} \quad (2.3)$$

It is clear through the above formulas, (2.2) and (2.3), that both molecular weight and strain rate influence the transition temperature T_{tr} , whereas the critical temperature T_{cr} is independent of molecular weight.

The mechanisms of crazing depend entirely on the magnitude of the maximum frictional force acting on the chain or fragments caused by the deformation process. As shown in Figure 1 by all the solid lines, at temperatures above T_{tr} , the maximum frictional force at the center of the chain is smaller than the force required to break the chain ($f_{\text{max}} < F$), and a craze grows by pure disentanglement (region I). Below T_{tr} , $f_{\text{max}} \approx F$, and chain scission occurs (region II). Any chains or chain fragments longer than L_{crit} under these drawing conditions will break, and those shorter than it will not. As temperature decreases further, the contribution to surface energy from chain disentanglement decreases until T_{cr} is reached. Below T_{cr} a craze grows by pure scission (region III), and no energy is dissipated in the chain disentanglement. At temperatures between T_{cr} and T_{tr} , the craze grows via a mixed scission and disentanglement crazing mode.

In Figure 1, the broken lines are the schematic surface energy of craze growth by pure scission or pure

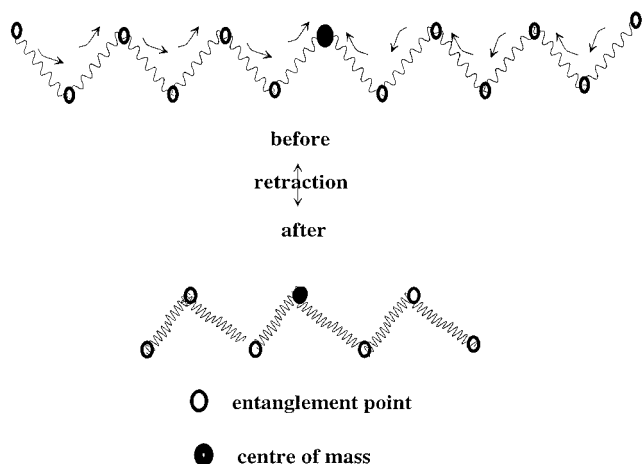


Figure 2. Entanglement loss by chain retraction within the active zone. Before retraction, the chain is stretched to a draw ratio of λ . Subsequently it may return toward its equilibrium contour length.

disentanglement. From a pure energy argument, there should only be one transition temperature T_i for a given molecular weight and strain rate. Above T_i , crazes grow by pure disentanglement and below it by pure scission. However, the scission process is force controlled (f_{\max}), unlike the disentanglement process which is energy controlled (f_{av}). Therefore, scission occurs at a higher temperature than T_i , in fact at T_{tr} , because at that point the frictional force is strong enough to break the backbone chain.

Disentanglement Effect

There has developed a tendency to distinguish between the deformation of material flowing directly into fibrils via the active zone from that of material initially *between* fibrils, which is said to experience “geometrically necessary entanglement loss”.¹¹ In fact it is not necessary to do this: all points in the active zone correspond locally to deformation fields which are of dominant extensional character. The main difference is that in regions above fibril centers the extensional direction is parallel to the fibril axis, while between fibrils it is parallel to the craze/bulk interface. Of course the magnitude of the local extension rates achieves its maximum between the fibrils near the separation point, which permits the flow into the fibrillar structure in the first place.

The physics of the “active zone” is still somewhat mysterious—the combination of large local surface area, high stresses and weak anisotropy of chains conspire locally to mobilize the otherwise glassy polymeric state. So the standard polymer-melt time scales, such as the Rouse time (the time scale for retraction of path length), are temporarily reduced from the effectively infinite values in the bulk to times comparable to experimental values in the active zone. This reduction permits the “disentanglement” necessary to flow into the craze—fibril geometry.

Now the accepted local picture of disentanglement in a polymer melt is that of *chain-retraction* within a “tube” or equivalent series of “slip-links” illustrated in Figure 2. Recovery toward the equilibrium entanglement path length of a chain destroys entanglements near its extremities. If the Rouse retraction time is reduced in the active zone permitting chains to disentangle, this condition must obtain throughout the active zone.

Complete retraction is prevented by the return of the material to a glassy state in the fibrils and consequent exponential regrowth of the relaxation times. That retraction is incomplete follows from the physical coupling between molecular deformation and mobility in the active zone: as molecules relax so the retraction time scale must return to its glassy value.

To study the influence of the mathematical functional form of the retraction dynamics on the average tension in the chain, special chain retraction dynamics must be assumed for stretched polymers below the glass transition temperature (T_g). We noted above that the mobility in the active zone is not sustained after relaxation of the high stresses generated by flow into the fibrils. A reasonable way to model this transition in mobility is to assume that the glassy environment prevents further retraction after one Rouse time τ_R . This criterion or something very like it is necessary to distinguish the active zone below T_g with a normal polymer melt above it. We will see in the following that its incorporation changes the calculated disentanglement energy by a significant factor. We assume that the glassy environment stops disentanglement beyond τ_R . As illustrated in Figure 2, the number of entanglements per chain at time $t = 0$ of the retraction is $n_e(0) = L/a$. When the chain retraction ceases ($t = \tau_R$), the number of entanglements per chain, $n_e(t)$, is $L/(\lambda a)$. The total entanglement loss per chain is $(\lambda - 1)L/(\lambda a)$.

The evidence of residual orientation in fibrils points to a useful mobilization/freezing criterion in the active zone as the attempted local strain of the network increases beyond its “natural draw ratio”, λ . Moreover, most material in the active zone is not deformed by more than this. This points to the local adjustment of dynamical time scales such that about one effective Rouse time occurs for material passing through the active zone. More than this would not give orientation in the fibrils, less would not permit disentanglement crazing at all.

We therefore propose that a generic history of a molecule in the active zone consists of (i) its local extension to a strain $\geq \lambda$ and (ii) its path length retraction including disentanglement for one active-zone Rouse time, followed by (iii) the freezing-in of the partially retracted state. Since most chains in the active zone suffer such a history, it will control quantities such as the average frictional force, f_{av} and thus the dissipation contribution to craze energies. It will also determine the maximum force in the chains, and thus the transition to scission-dominated crazing.

The functional form of the “activated retraction” with time also has a quantitative effect, which we illustrate by the following two cases, which take different assumptions.

Linear Retraction. First as in the previous theory¹⁰ we chose a simple linear retraction function. The number of entanglements per chain $n_e(t)$ decreases from its original value $n_e(0)$ as the chain retracts from a draw ratio of λ to its equilibrium length:

$$\frac{n_e(t)}{n_e(0)} = \begin{cases} \frac{1}{1 + (\lambda - 1)(t/\tau_R)} & t \leq \tau_R \\ 1/\lambda & t > \tau_R \end{cases} \quad (3.1)$$

The ratio of the average number of entanglements per chain in the retraction process over the original number is therefore calculated to be

$$\frac{\langle n_e(t) \rangle_t}{n_e(0)} = \frac{\ln \lambda}{\lambda - 1} = 0.462 \quad \text{for } \lambda = 4 \quad (3.2)$$

Rouse Retraction. To explore the consequences of a more realistic functional form of chain retraction dynamics, we have also explored the consequences of an exponential relaxation form for chain retraction, as in the Rouse mode, to compare with Plummer and Donald's theory.¹⁰ For simplicity we have used a single relaxation time for the tube length:¹³

$$L(t) = L[1 + (\lambda - 1)e^{-t/\tau_R}] \quad (3.3)$$

The number of entanglements per chain at time t compared to its original value is

$$\frac{n_e(t)}{n_e(0)} = \frac{L(t)}{\lambda L} \quad (3.4)$$

and the ratio of the average number of entanglements per chain in the retraction process over the original number

$$\frac{\langle n_e(t) \rangle_t}{n_e(0)} = 0.632 + \frac{0.368}{\lambda} = 0.724 \quad \text{for } \lambda = 4 \quad (3.5)$$

We have seen that the average force per chain, f_{av} , is proportional to n_e^2 (eq 1.4), and so it follows that the loss of entanglements during chain retraction results in a reduction of $0.462^2 = 0.21$ or $0.724^2 = 0.5$ in the average force according to linear or exponential dynamics, respectively. Exponential retraction dynamics are considered to be more realistic and are used in the following calculations. (We note that Plummer and Donald¹⁰ assumed linear retraction dynamics and that $f_{av} \propto \langle n_e \rangle$ resulting in a reduction in force by a factor of 0.46, fortuitously close to the value of 0.5 used here).

The experimental time scale relative to τ_R is vitally important in the chain retraction process as discovered in the orientation relaxation of monodisperse linear and star polystyrenes.¹⁴ Although the chain retraction process on time scale τ_R modifies the average chain tension, τ_R does not appear in the final results because by our assumptions $\tau_R \approx \tau_{exp}$, where τ_{exp} is the experimental time scale ruled by k^{-1} , and self-adjusts in the active zone to permit the necessary partial retraction of the chains.

Energy Analysis. The total surface energy required to propagate the craze void of the polymer is composed of the van der Waals surface energy (γ), which is 0.04 N/m for polystyrene,^{10,11} the energy to cause chain scission (Γ_s), and the energy needed to disentangle the chains or fragments (Γ_d).

$$\Gamma = \gamma + \Gamma_s + \Gamma_d \quad (4.1)$$

In the mixed crazing regime, any entangled strand of molecular weight M_e will either break (with probability Y) or disentangle (with probability $(1 - Y)$). Therefore, we may distinguish the consumption of energy by scission and disentanglement energy per unit area as follows:

$$\Gamma_s = \frac{1}{4}avUY \quad (4.2)$$

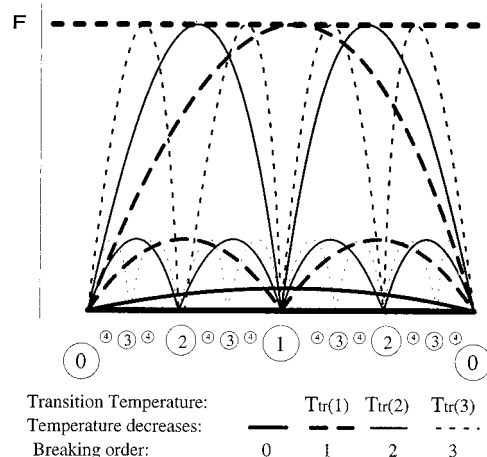


Figure 3. Discrete crazing model. Schematic of scission events and force profiles are given vs path contour variable along the chain for four temperatures. Numbers note the position and order of scission. Whenever the parabolic force profile reach f_{max} (upper dashed line) at the chain midpoint, it breaks there, immediately adjusting the force profile in the resulting two subchains.

$$\Gamma_d = \frac{avb}{2}(1 - Y)\langle f_t \rangle \quad (4.3)$$

Here ν is the entanglement density, $avb/2$ is the strand density per unit area, $\langle f_t \rangle$ is the average force needed to disentangle a chain or fragment.

The final piece of information needed to calculate the force in the disentangling fragments is their molecular weight M_{frag} . Within our model, M_{frag} is actually distributed between M_{crit} and $M_{crit}/2$ because of the hierarchical scission process illustrated in Figure 3. If the *penultimate* scission event on a chain leaves fragments of molecular weight *just greater* than M_{crit} , the final fragments will be of approximately $M_{crit}/2$. On the other hand, the penultimate fragments may be nearly as large as $2M_{crit}$, leaving fragments of nearly M_{crit} after all the scission events. This process leads to the upper and lower bounds in our calculation of craze energies in the mixed scission/disentanglement regime (see below).

In the mixed crazing regime, it is assumed that the maximum force to disentangle the chain of molecular weight M_{crit} equals the force to break it (F).^{10,11} We recall that the average force to disentangle the chain is two-thirds of the maximum frictional force which equals $U/2b$ and that our considerations of the entanglement loss effect on average force gave a factor of 0.724^2 , obtained using exponential retraction dynamics. The lengths of the broken fragments are between $M_{crit}/2$ and M_{crit} . The average force is proportional to the square of chain length, which leads to the last term of the following formula:

$$\langle f_t \rangle = \frac{U}{2b} \left(\frac{2}{3} \right) 0.724^2 \begin{cases} 1 & M_{frag} \approx M_{crit} \\ 1/4 & M_{frag} \approx M_{crit}/2 \end{cases} \quad (4.3a)$$

At a given strain rate, when temperature decreases, the critical molecular weight, M_{crit} decreases. At T_{tr} , M_{crit} equals M and the chains break in the middle. The number of strands per chain is M/M_e . The probability of scission per entangled strand is $1/(M/M_e)$. In the mixed crazing regime ($M > M_{crit} > M_e$), the number of scission events per chain is M/M_{crit} . The probability of

scission for one strand is $(M/M_{\text{crit}})/(M/M_e)$, which is M_e/M_{crit} . Therefore, the general scission probability for a strand takes the following form:

$$Y = \begin{cases} 1 & M_{\text{crit}} \leq M_e \\ M_e/M_{\text{crit}} & M_e < M_{\text{crit}} \leq M \\ 0 & M_{\text{crit}} > M \end{cases} \quad (4.3b)$$

From the strand scission probability analysis, (4.3b), it is clear that when the critical molecular weight equals M_e , the probability that every strand is broken is equal to 1. That means no strand needs to be disentangled. This corroborates our argument that T_{cr} occurs when M_{crit} equals M_e instead of $2M_e$.

For pure disentanglement, Γ can be calculated by (4.3) plus the van der Waals energy, where Y equals zero and the average force can be calculated by formulas 1.4 and 3.5.

Discrete Model

In the real situation, Y is discrete because the number of scission events per chain is discrete. At the temperature range where M_{crit} is between M and $M/2 + \epsilon$ (ϵ is a small number close to zero), chain scission only happens once, not as described by (4.3b) as a continuous change from 1 to 2. Γ_d is defined by the length of the fragments after the first scission event (molecular weight $M/2$). Therefore, Γ_d is higher than that calculated from molecular weight $M_{\text{crit}}/2$ but lower than that calculated from M_{crit} (as calculated by (4.3a)). Formula 4.3a actually defined the lower boundary of Γ in the mixed regime when the bracket option is $1/4$ and the upper boundary when the bracket option is 1.

The discrete model for crazing based on this velocity profile (general tube model) can be worked out following the theory we developed so far. Figure 3 illustrated the frictional force built up along the chain at a given strain rate as temperature decreases and the chain break-down when f_{max} reaches F at a transition temperature. As shown in Figure 3, for a polymer of molecular weight M (length from 0 to 0 in the graph) at temperatures above T_{tr} (noted as the first transition temperature, $T_{\text{tr}}(1)$ in the discrete model), f_{max} in the middle of the chain is lower than the force required to break the chain, F . At the same experimental strain rate, as the temperature decreases, f_{max} increases continually until reaching F at temperature $T_{\text{tr}}(1)$, and the chain breaks in the middle (point 1 in the graph). Two fragments of molecular weight $M/2$ (length from 0 to 1) were formed. The new force profiles along the first broken fragments are shown by the thick broken curves. The maximum force acting on the first-order broken fragment is $1/4$ of F at $T_{\text{tr}}(1)$ according to formula 1.3.

As temperature drops further, the frictional force acting on the first order fragment increases. The maximum force acting on the first order fragments increases gradually from $F/4$. At the same time, M_{crit} decreases from M . However, the secondary scission will not occur until M_{crit} decreases to reach $M/2$. At the temperature range that M_{crit} decreases from M to $M/2$, the fragment length is a constant ($M/2$). However, the energy required to disentangle it, as temperature is reduced, increases because of its decreased mobility or increased monomer friction coefficient. The maximum force acting on the first-order fragments increases to F as M_{crit} decreases from M to $M/2$, when the secondary transition temperature ($T_{\text{tr}}(2)$) was reached (medium

Table 1. Key Parameters in the Discrete Model for Crazing

T_{tr}	M_{crit}	n_s	Y
$T_{\text{tr}}(1)$	M		
\downarrow			
$T_{\text{tr}}(2)$	$M/2$	1	M_e/M
\downarrow			
$T_{\text{tr}}(3)$	$M/4$	3	$3M_e/M$
\downarrow			
$T_{\text{tr}}(4)$	$M/8$	7	$7M_e/M$
\downarrow			
\dots	\dots	15	$15M_e/M$
$T_{\text{tr}}(n)$	$M/2^{n-1}$	\dots	\dots
\downarrow			
$T_{\text{tr}}(n+1)$	$M/2^n$	$2^n - 1$	$(2^n - 1)M_e/M$

solid lines). At $T_{\text{tr}}(2)$, the first-order fragments break in the middle (points marked 2 in the graph) and secondary fragments are formed with molecular weight $M/4$ (length from 0 to 2). The new force profiles along secondary fragments are shown by the medium solid lines too. The maximum force acting on the secondary fragments is also $F/4$ at $T_{\text{tr}}(2)$.

This force build-up and fragments break-down process will progress until temperature reaching T_{cr} . As shown in Table 1, the transition temperatures for the first, second, third, ..., and the n th scission event per chain can be calculated from formula (2.2) corresponding to molecular weight $M, M/2, M/4, \dots, M/2^{n-1}$ respectively. The number of scission events per chain between transition temperatures $T_{\text{tr}}(1)$ and $T_{\text{tr}}(2)$, $T_{\text{tr}}(2)$ and $T_{\text{tr}}(3)$, $T_{\text{tr}}(3)$ and $T_{\text{tr}}(4)$, and ... $T_{\text{tr}}(n)$ and $T_{\text{tr}}(n+1)$ are 1, 3, 7, ..., $2^n - 1$, respectively. The probabilities of scission for a strand are $[1, 3, 7, \dots, 2^n - 1] \times M_e/M$ at the respective temperature range. The lower temperature cutoff of the mixed craze regime is defined by the critical temperature.

The craze surface energy consumed in disentanglement is calculated using (4.3). In the discrete model the real fragment molecular weight $M/2^{n-1}$ is used to calculate the disentanglement energy instead of M_{crit} or $M_{\text{crit}}/2$ which was previously used or suggested in the literature.^{10,11} We will see below that the temperatures at which the number of scission events per chain suffers a discontinuity are marked by a cusp-like discontinuity in the craze surface energy. Also the energy to disentangle the fragments is calculated using (1.4) and (4.3) instead of approximated by using (4.3a). It is worth noting that in the discrete model, $M_{\text{crit}} > M_{\text{frag}} = M/2^{n-1} \geq M_{\text{crit}}/2$. It is now clearer that previous theories only predicted the upper or lower boundaries of the craze growth surface energy in the mixed crazing regime as defined by (4.3a) in this model.

Results and Discussion

In this section, our experimental results and data from the literature^{10,11} are used to calculate the craze growth surface energy vs temperature between 0 and 100 °C. This range of temperature covers the whole craze growth mechanism transition regime for polystyrene.

Experimental Results. The stress to craze for each drawing condition was calculated using experimental Young's moduli and the strains to craze at different temperatures assuming a linear relationship between stress and strain to craze.¹⁰

In Figure 4 we present the strain to craze for monodisperse linear PS L110k at strain rates of 10^{-3}

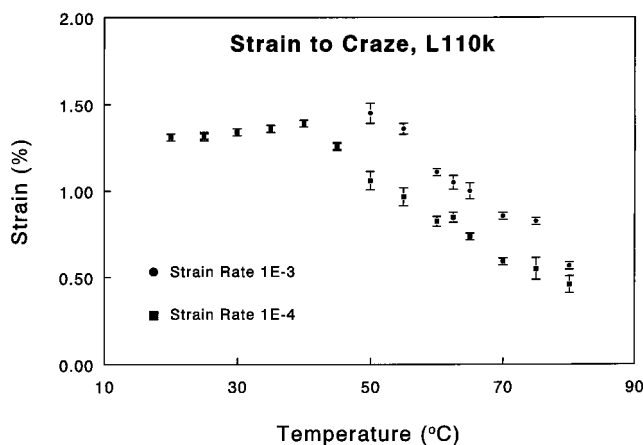


Figure 4. Strain to craze for linear PS 110k at strain rates 10^{-3} s^{-1} (circles) and 10^{-4} s^{-1} (squares) at temperatures between 20 and 80 °C.

and 10^{-4} s^{-1} in the temperature range of 20 to 80 °C. The error bars represent the standard error in the mean of 6–10 samples for each temperature/strain rate combination. At room temperature the stresses deduced from strain to craze for L110k are about 37 MPa at both strain rates. Temperature rises and at 42 °C the stress to craze at 10^{-4} s^{-1} begins to decrease. This reduction occurs at a higher temperature (52 °C) in the higher strain rate (10^{-3} s^{-1}) experiment. The temperature dependence of the crazing strain for the experiments at different strain rates are almost the same in the high-temperature region. Noticeably, there is a small peak in crazing strain in the low strain rate experiment (10^{-4} s^{-1}) at 62.5 °C. For the experiment at high strain rate (10^{-3} s^{-1}), there is apparently no peak but instead a plateau is seen around 70–75 °C. A small number (two) of relatively sharp peaks (cusps) in the craze surface energy, and so by implication in the crazing strain at each strain rate, are predicted by the present theory and so the feature at 62.5 °C (10^{-4} s^{-1}) requires some further discussion. To establish the existence of the peak from these samples alone would need a significant increase in the number of temperatures used for experiments in their vicinity. However, in addition to the theoretical expectation, data to be published on monodisperse star polymers¹² (of comparable total span molecular weight) at two different strain rates also suggest the existence of a small peak in the crazing strain, as do independent data on PMMA.¹⁷

Comparison with Theory. The craze surface energy from our experiments was obtained using the formula^{10,11}

$$\Gamma_{\text{exp}} = \frac{D_0 E \epsilon_c}{8} \quad (5)$$

where ϵ_c is the strain to craze as shown in Figure 4, D_0 is the craze fibril spacing and E is the Young's modulus.¹⁰ In ref 11 a multiplicative factor β of order 1 was included in eq 5. However, β may be calculated from the crazing stress at room temperature and from the pure van der Waals regime. We found a value consistently close to unity. The molecular weight is very similar for our samples and L127k.¹⁰ Because only a very weak molecular weight dependence upon D_0 value was observed,¹⁰ we used the temperature dependent D_0 values of L127k directly for our samples.

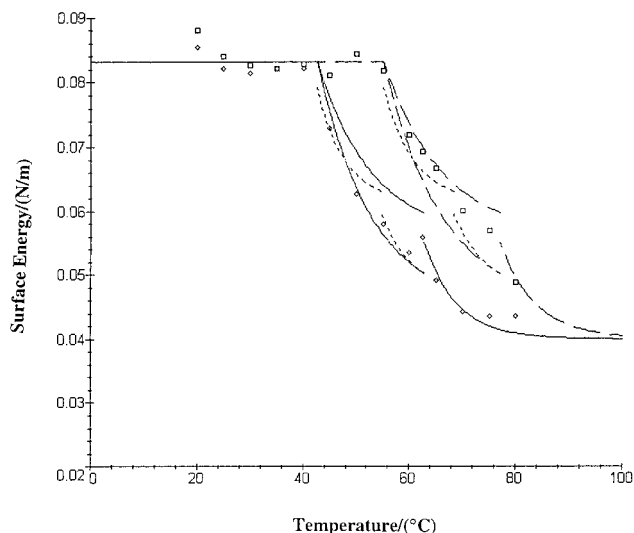


Figure 5. Calculated surface energy for linear PS 110k at strain rates 10^{-3} s^{-1} experimental (square) and theory (solid line); and 10^{-4} s^{-1} experimental (diamond) and theory (broken line) at temperatures between 20 and 80 °C. Dotted lines are calculated from the discrete model of scission.

From our previous analysis, for a given molecular weight, strain rate and temperature, a critical molecular weight can be calculated using (2.1). In formula 2.1 and the following calculation, the functional form for the temperature dependence of the monomer frictional coefficient in the melt state was used in the craze growth process in the absence of direct data for the crazing process.^{10,11} However, recent experiments^{15,16} observed that when the film thickness was below 150 nm for polystyrene, the effect of the free surface became substantial and films did not behave like typical solids. In light of these experimental results, keeping in mind that the craze fibril diameter and void diameter are typically 20 nm for polystyrene, the free surface effect may increase the chain mobility significantly. The mobility of chains in the active zone of a craze may well be close to that in the melt state.

Below T_{cr} , the craze surface energy can be calculated by (4.2) for the pure scission crazing ($Y = 1$). Above T_{tr} , formula 4.3 can be used for the pure disentanglement crazing ($Y = 0$). Between the critical and transition temperature, the craze surface energy can be calculated from (4.3a) and (4.3b) for the disentanglement and scission mixed crazing.

In Figure 5, the experimental results include L110k drawn at 10^{-3} and 10^{-4} s^{-1} . Both experiments showed a peak in the craze surface energy (see discussion of Figure 4, above). At the lower strain rate (10^{-4} s^{-1}) this peak is at 62.5 °C. For the experiment at the higher strain rate (10^{-3} s^{-1}), the peak occurs around 75 °C. The theoretical curves were fitted by fixing the strain rate ratio of the two experiments, i.e., assuming a linear relationship between the velocity constant k in formula 1.1 and the experimental strain rate. There are no other adjustable parameters in this calculation.

The results from the discrete model were shown in Figure 5 as dotted lines and that from the lower boundary of general tube model as solid lines. It is clear from Figure 5 that the agreement between our calculations and the experimental results is generally very good. At each strain rate the following features of the experimental data are correctly described by this theory. At low temperatures the surface energy, Γ is indepen-

dent of both temperature and strain rate (scission-dominated crazing). With increasing temperature there is a sudden decrease in Γ at a critical temperature, T_{cr} , followed by a region where Γ decrease more slowly (mixed mode crazing). There is a further discontinuous change in Γ at a transition temperature T_{tr} and then a final region of disentanglement crazing above T_{tr} . It should be noted that the theoretical calculations correctly predict the observed variation in T_{tr} and T_{cr} with strain rate. Furthermore the theory predicts an increase in Γ at T_{tr} , which is clearly shown by the experimental data at the lower strain rate. The small discrepancies at the higher strain rate may result from the failure of the local strain rate to follow that of the bulk, or from a fluctuation in the local chain velocity about its mean.

As the strain rate increases, the transitions from pure scission to scission and disentanglement mixed crazing, and from mixed crazing to pure disentanglement are shifted to higher temperatures. It is easy to see that at a high strain rate, there may be no pure disentanglement regime. At still higher strain rates, only pure scission crazing occurs.

The "block and tackle" theory^{9,10} relies on multiple crossing of the chain across the separating plane. A relatively high molecular weight is required for the "block and tackle" theory to work. However, the previous studies showed a reasonable fit between L127k experimental data and "block and tackle" theoretical results. This implies that the underlying physics does not require a very high molecular weight for the single chain model to work. Our calculation from the general tube model for crazing supported this claim.

Our theory fits our experimental results of L110k drawn at 10^{-3} and 10^{-4} s⁻¹ generally well. It is of interest to compare the calculations from our theories with the previous theories^{10,11} and experimental results. The agreement between the experimental data and theoretical calculations for high molecular weight linear polystyrene was previously particularly unsatisfactory. So these data provide a particularly useful test of the modifications we propose in this paper.

On the basis of the k value obtained in Figure 5 and the assumption of a linear relationship between the experimental strain rate and the k value in the basic model, we calculated the results for L1150k drawn at 4×10^{-6} s⁻¹ without any adjustable parameters. In Figure 6, the experimental results of linear 1150k drawn at 4×10^{-6} s⁻¹ are presented (circles).¹⁰ The solid lines are calculated from the general tube model of this paper. In the mixed crazing regime, the upper and lower boundaries were shown, which agreed with the experimental data reasonably well. Dotted lines are from the discrete model, which mapped some of the details of the experimental data. The overall fit of the current theory is improved from that of the previous theories, particularly at low temperatures. Our predicted transition temperature is the same as the experimental results and is better than previous theoretical calculations. Still the critical temperature predicted by this calculation is higher than the experimental data, though improved from previous theories.

Our critical temperature argument is also supported by the experimental fact that the temperature range of the mixed mode is wider than the previous theoretical predictions which used $2M_e$ to calculate T_{cr} . Using M_e to calculate the critical temperature rather than $2M_e$

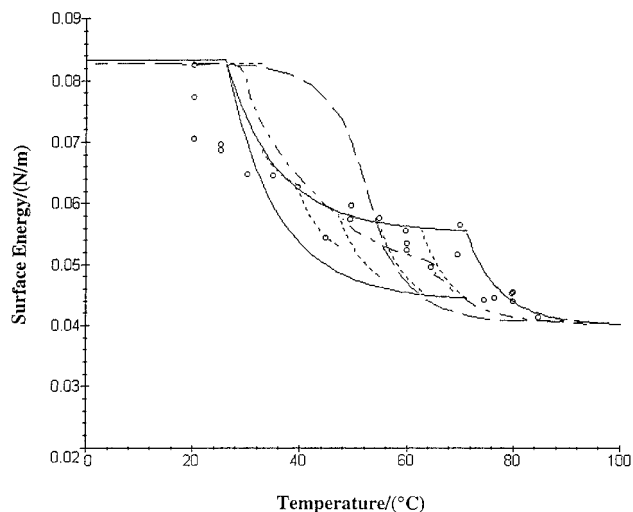


Figure 6. Calculated craze growth surface energy of L1150k drawn at 4×10^{-6} s⁻¹ (circle) [10]; this theory: (—) continuous; (---) discrete; (- - -) Plummer and Donald's; (- - -) Kramer's.

shifts the pure scission regime to a lower temperature, which is in line with the experimental data.¹⁰

Disentanglement is the energetically favored mechanism in the mixed crazing regime. This can be clearly seen from formula 4.3a. First, the entanglement loss caused by chain retraction decreased the energy to disentangle a chain by about 50% for PS. Furthermore, the energy required to break a chain is associated with f_{max} , whereas the energy required to disentangle a chain is associated with f_{av} on the chain. The latter is only two-thirds of the former. If these two effects are combined, in the mixed crazing regime, the energy to break a strand is three times that required to disentangle a strand.

The discontinuity in the craze surface energy curve at the transition temperature is a general phenomenon in glassy polymers. It has been observed recently in systems such as PES¹⁰ and PMMA.¹⁷ Going back to Plummer and Donald's experimental results (Figure 6), we can see that they also support the possibility of a maximum at their respective transition temperature. Their suggestion that the maxima derive from a cross-over between crazing mechanisms may be explored within the present model.

Going back to Figure 1, it is now clear that at T_{tr} , the transition temperature from force balance, it is generally true that the craze growth surface energy via mixed crazing differs from that via pure disentanglement. In other words there is a potential discontinuity in Γ curve at T_{tr} . The discontinuity of craze surface energy can be calculated from (4.3) using the discrete model

$$\Delta\Gamma \equiv \Gamma_{dis} - \Gamma_{mix} = \frac{avU}{24} \left\{ 3 \left(\frac{\langle n_e(t) \rangle_t}{n_e(t)} \right)^2 - \frac{M_e}{M} \left[6 - \left(\frac{\langle n_e(t) \rangle_t}{n_e(t)} \right)^2 \right] \right\} \quad (6)$$

For λ equals 4 (in the case of polystyrene), $\Delta\Gamma$ is zero for polystyrene with a molecular weight of $11M_e/3 \approx 64\,500$. For polymers with molecular weights higher than 64 500, the pure disentanglement crazing surface energy is higher than that of the mixed mode of crazing at T_{tr} (thick solid lines). For a very high molecular

weight PS, the difference is about 0.011 N/m. For polymers of molecular weight lower than 64 000, the pure disentanglement crazing surface energy is lower than that of the mixed mode of crazing (thick broken lines) and the difference is small. The lowest is for a polymer of molecular weight $2M_e$, and the difference is about 0.009 N/m. In practice, this discontinuity will be smeared out by the fragment molecular weight distribution at temperatures close to T_{tr} in the mixed crazing regime.

Combining Figures 5 and 6, it is not difficult to see that the craze growth surface energy is molecular weight independent in the mixed crazing regime, even though it is strain rate dependent. The molecular weight only changes the position of transition temperature. This is partly observed in the experiments near $T_{tr}^{10,17}$ (see Figures 5 and 6).

The transition temperature at high strain rate predicted here in Figure 5 is still slightly higher than the experimental value, attributed to the center of mass motion of the linear molecules, which will be analyzed in the following paper of this series.¹²

Conclusions

The strain rate effect on the surface energy and crazing mechanisms for monodisperse linear polystyrene has been studied both experimentally and theoretically. A satisfactory fit between theory and experimental results has been obtained.

We have demonstrated that a general tube model for crazing is valid for fairly low molecular weight systems. This theory provided an improved quantitative description of the features in the craze growth surface energy vs temperature curve in comparison with previous theories and the calculations were in fine agreement with experimental data.

Entanglement is lost by the chain retraction process. The functional form of the retraction dynamics is important for the craze growth surface energy calculation, and an exponential dynamics gives results close to the experimental data.

The critical temperature, the highest temperature for pure scission crazing, corresponded to critical molecular weight equals the entanglement molecular weight. It depends on the experimental strain rate but is independent of the molecular weight. The transition temperature, the lowest temperature for pure disentanglement, depends on both the molecular weight and strain rate. Disentanglement is the energetically favored crazing mechanism in the mixed crazing regime.

Using the general tube model for crazing, a discrete model has been developed. The calculations clearly showed that previous theories predicted only the lower and upper boundaries of the craze growth surface energy in the mixed crazing regime. Real fragment lengths were used, instead of the critical molecular weight or half of the critical molecular weight as used in previous theories, to calculate the disentanglement energy in the mixed crazing regime, and details of the craze growth surface energy were obtained and found to agree with the experimental data. We have also demonstrated that the discontinuity in the craze growth surface energy at the transition temperature is a universal phenomenon for glassy polymers. The sign and magnitude of the discontinuity depends on the molecular weight of the polymer. The discontinuity is attributed to the difference between the maximum and

average frictional force acting on the chain and the fact that scission is associated the former whereas disentanglement is linked with the latter.

It remains for one to explain the persisting quantitative discrepancies between those data and the theory as it stands. One appealing suggestion¹⁴ is to attribute them to curvilinear motion of the centers-of-mass of the entangled chains in the active zone. This conjecture could be verified experimentally by suppressing such motion by molecular architecture. Star-shaped molecules will have their central monomers fixed within the entanglement network. We will follow up this suggestion both experimentally and theoretically in the following paper of this series.

Acknowledgment. We thank the EPSRC (U.K.) for financial support.

Appendix: Glossary of Symbols

T_{tr}	transition temperature from disentanglement to mixed-mode crazing
T_{cr}	transition temperature from mixed-mode to scission crazing
M_{crit}	critical molecular weight for chain scission (function of rate and temperature)
T_g	glass transition temperature
f_{max}	maximum chain tension
f_{av}	average chain tension
v	relative velocity between a point on a chain and its surroundings (tube)
k	rate of change of v with arclength coordinate s
s	arclength coordinate along a chain
\mathbf{K}	deformation-rate gradient tensor
ζ	monomeric friction constant
E	activation energy responsible for the monomeric friction
L	primitive path length of polymer chain
L_{crit}	primitive path length corresponding to M_{crit}
U	energy required to break a polymer chain.
b	monomer length
M_e	entanglement molecular weight
M_0	monomer molecular weight
λ	maximum draw ratio
n_e	number of entanglements per chain
τ_R	Rouse retraction time
Γ	craze surface energy
Y	Probability of strand scission
ϵ_c	strain to craze
D_0	craze fibril spacing

References and Notes

- (1) de Gennes, P. G. *J. Phys. Fr.* **1989**, 50, 2551.
- (2) Ji, H.; de Gennes, P. G. *Macromolecules* **1993**, 26, 520.
- (3) O'Connor, K. P.; McLeish, T. C. B. *Polymer* **1992**, 33, 4314.
- (4) Brown, H. R. *Annu. Rev. Mater. Sci.* **1991**, 21, 463.
- (5) Creton, C. F.; Brown, H. R.; Deline, V. R. *Macromolecules* **1994**, 27, 1774.
- (6) Washiyama, J.; Kramer, E. J.; Creton, C. F.; Hui, C.-Y. *Macromolecules* **1994**, 27, 2019.
- (7) Prentice, P. *Polymer* **1983**, 24, 344.
- (8) Berger, L. L.; Kramer, E. J. *Macromolecules* **1987**, 20, 1980.
- (9) McLeish, T. C. B.; Plummer, C. J. G.; Donald, A. M. *Polymer* **1989**, 30, 1651.
- (10) Plummer, C. J. G.; Donald, A. M. *Macromolecules* **1990**, 23, 3929.
- (11) Kramer, E. J.; Berger, L. L. *Adv. Polym. Sci.* **1990**, 90/91, 1.

- (12) Han, H. Z. Y.; McLeish, T. C. B.; Duckett, R. A.; Donald, A. M.; Ward, N. J.; Johnson, A. F. *Macromolecules*, to be submitted for publication.
- (13) Doi, M.; Edwards, S. F. *The theory of polymer dynamics*, Oxford, England, 1986.
- (14) Han, H. Z. Y.; Duckett, R. A.; McLeish, T. C. B.; Ward, N. J.; Johnson, A. F. *Polymer* **1997**, 38, 1545.
- (15) Keddie, J. L.; Jones, R. A. L.; Cory, R. A. *Europhys. Lett.* **1994**, 27, 59.
- (16) Frank, B.; Gast, A. P.; Russell, T. P.; Brown, H. R.; Hawker, C. *Macromolecules* **1996**, 29, 6531.
- (17) Levitt, R. Ph.D. Thesis, Cambridge University, 1996.

MA961896O